Third-order optical measurements of porphyrin compounds using Dark-field and D4σ-Z scan imaging techniques

Georges Boudebs, C. Cassagne, H. Wang, Jean-Luc Godet, C.B. de Araújo

▶ **To cite this version:**

Georges Boudebs, C. Cassagne, H. Wang, Jean-Luc Godet, C.B. de Araújo. Third-order optical measurements of porphyrin compounds using Dark-field and D4σ-Z scan imaging techniques. Journal of Luminescence, 2018, 199, pp.319-322. 10.1016/j.jlumin.2018.03.055 . hal-02442799

HAL Id: hal-02442799
https://hal.science/hal-02442799

Submitted on 16 Apr 2021

HAL is a multi-disciplinary open access archive for the deposit and dissemination of scientific research documents, whether they are published or not. The documents may come from teaching and research institutions in France or abroad, or from public or private research centers.

L'archive ouverte pluridisciplinaire **HAL**, est destinée au dépôt et à la diffusion de documents scientifiques de niveau recherche, publiés ou non, émanant des établissements d'enseignement et de recherche français ou étrangers, des laboratoires publics ou privés.

Distributed under a Creative Commons Attribution 4.0 International License

Third-order optical measurements of porphyrin compounds using Dark-field and D4σ-Z scan imaging techniques

G. Boudebs[1,*] , C. Cassagne[1], H. Wang[1], J.-L. Godet, and C. B. de Araújo[2]

[1] *Laboratoire de Photonique d'Angers, LPHIA, EA 4464, SFR MATRIX, UNIV Angers, 2 Boulevard Lavoisier, 49045 Angers France.*
[2]*Departamento de Física, Universidade Federal de Pernambuco, 50670-901 Recife, PE, Brazil*

ARTICLE INFO

Keywords: Optical properties. Organic compounds. Nonlinear response. Z-scan

ABSTRACT

The newly introduced imaging techniques D4σ and Dark-field Z-scan (DFZ-scan) are very much appropriate to measure the third-order nonlinear (NL) refractive index in the presence of high nonlinear absorption (NLA) in condensed matter. To demonstrate the large potential of both techniques we prepared and characterized porphyrins solutions in chlorobenzene and report here on the NL optical properties of 5,10,15,20-Tetraphenyl-21H,23H-porphyrin (TPP), 5,10,15,20-Tetraphenyl-21H,23H-zinc porphyrin (ZnTPP), 5,10,15,20-tetraphenyl-21H,23H-porphyrin cobalt(II) (CoTPP) and 5,10,15,20-tetrakis(4-methoxyphenyl)-21H,23H-porphyrin cobalt(II) (MCoTPP). The measurements were performed with a laser delivering low repetition rate linearly polarized single picosecond pulses at 1064 nm and 532 nm.

1. Introduction

Because of the large discrepancy found in the literature related to third-order optical nonlinear (NL) coefficients an unbiased comparison of different materials sometimes is very difficult. Hence, development of new NL techniques is still relevant and subject to active research [1, 2, 3] to find simple and sensitive ways to measure the optically induced NL refraction (NLR) despite of the presence of relatively high NL absorption (NLA). Therefore, the newly introduced imaging techniques: DFZ-scan [4] and D4σ-Zscan [5, 6] are applied here to demonstrate their ability to measure the third-order NL refractive index, n_2, in presence of large NLA coefficient, β, as it is often the case with organic materials. The experiments were performed by determining the transmitted laser beam waist relative variation (BWRV) using D4σ intensity profile measurements combined with the Z-scan method [7] in a 4f-system for different porphyrins (Pphs) dissolved in chlorobenzene. Using DFZ-scan we determined the sign and the magnitude of n_2 and β even at relatively high Pphs concentration. The experiments allowed to test all cases of positive and negative NLR and NLA coefficients. Although the synthesis and experimental NL optical characteristics of Pphs have been reported by several groups, the interest in these materials has been renewed due to their useful optical limiting properties (see for example [8, 9, 10, 11, 12] and references therein) here we provide accurate data for some Pphs thanks to the application of D4σ and DFZ-scan.

The unique electronic, optical and biochemical properties [13] as well as the high stability and architectural flexibility of Pph compounds provide a very good basis to finely tune their optical response. Moreover, the ability of Pph molecules to capture light allows their use in sensors based on optical waveguides, frequency converters, and devices for transmission and storage of information [14]. All Pphs have π-conjugated structures and, in general, they exhibit strong NLA and large NLR. In particular, due to the large NL response, the metalloporphyrins have been proposed for optical limiting and all-optical switching [15] in different optical regimes because, in addition to their highly conjugated structure, both metal-to-ligand and ligand-to-metal charge transfer, lead to intramolecular electron delocalization that enhances the molecule hyperpolarizability. The ability to present large NL response in fast and slow timescales (from the ns to the fs regimes) makes the Pphs particularly attractive for photonics. Therefore, characterizing their NL optical properties and identifying the variations in the NL response due to the change of the metal center is of large interest in order to optimize the materials for optical limiting and/or optical switching applications.

2. Experimental section

Commercially available (Sigma Aldrich Co.) Pphs powders were dissolved in chlorobenzene with concentrations varying from 10^{-4} to 10^{-3} M. The NL optical measurements were carried out using linearly polarized 17 ps pulses at 1064 nm and its second harmonic at 532 nm (12 ps), respectively, at 10 Hz repetition rate. The liquid suspensions were contained in 1 mm thick quartz cells.

As mentioned before two techniques were used: DFZ-scan and D4σ-Z-scan. With the D4σ-Z-scan method, the images of a circular aperture at the entry of the system (object plane) are recorded by a single-shot CCD camera located in the image plane of a 4f setup as a function of the sample position that is moved around the focal plane. The open-aperture Z-scan normalized transmittance was numerically processed from the acquired images allowing for simultaneous measurements of NLR and NLA coefficients. However, unlike the traditional closed-aperture Z-scan method, in the D4σ technique the

* Corresponding author.
E-mail address: georges.boudebs@univ-angers.fr (Georges Boudebs)

n_2 value is extracted from the acquired CCD images by measuring the BWRV in the image plane. On the other hand, the β value is determined using the usual open-aperture Z-scan procedure. The determinations of n_2 and β are supported with simulations of image formation inside the 4f system [6]. The measurement procedure is built to consider the response of the material described by an effective cubic nonlinearity characterized by n_2 and β. The relatively short picosecond pulses at low-repetition rate ensure that the contributions of thermal effects due to optical absorption are negligible. In these conditions, the transmittance of the sample is described by:

$$T(z,u,v)=\left[1+q(z,u,v)\right]^{-1/2}\exp\left[j\Delta\phi_{NL}^{eff}(z,u,v)\right] \quad (1)$$

where $\Delta\phi_{NL}^{eff}(z,u,v)=2\pi n_2 L I_{eff}(z,u,v)/\lambda$ is the NL phase-shift, $q(z,u,v)=\beta L I(z,u,v)$ and $I_{eff}(z,u,v)=I(z,u,v)\log\left[1+q(z,u,v)\right]/q(z,u,v)$ is the effective intensity. As an illustration of our results, the NLR behavior of TPP and ZnTPP (10^{-3} M) are shown in Figures 1(a) and 1(b), respectively; the data were obtained at 532 nm with 2.1 GW/cm^2. The BWRV profile with the peak after the valley indicates that the TPP presents a negative n_2 exhibiting self-defocusing at this wavelength. Notice that the BWRV trace has opposite symmetry in comparison with the Z-scan technique. The open-aperture Z-scan data, presented as insets of both figures, illustrate the NLA behavior. The effective two-photon absorption (2PA) model (Eq. (1)) shows very good agreement between the experimental results and the numerical calculated traces. In Fig. 1(a) the blue lines represent the best fit corresponding to $n_2=(-2.7\pm0.5)\times10^{-18}\text{m}^2/\text{W}$ and $\beta=(5.5\pm0.8)\text{cm/GW}$ for TPP. The same applies to Fig. 2(b) that shows the results corresponding to $n_2=(1.7\pm0.3)\times10^{-18}\text{m}^2/\text{W}$ and $\beta=(7.8\pm1.0)\text{cm/GW}$ for ZnTPP. These results illustrate clearly the influence of Zn on the NL response at 532 nm: (i) the sign of n_2 is positive for ZnTPP while it is negative for TPP; (ii) the 2PA coefficient of ZnTPP is larger than in TPP.

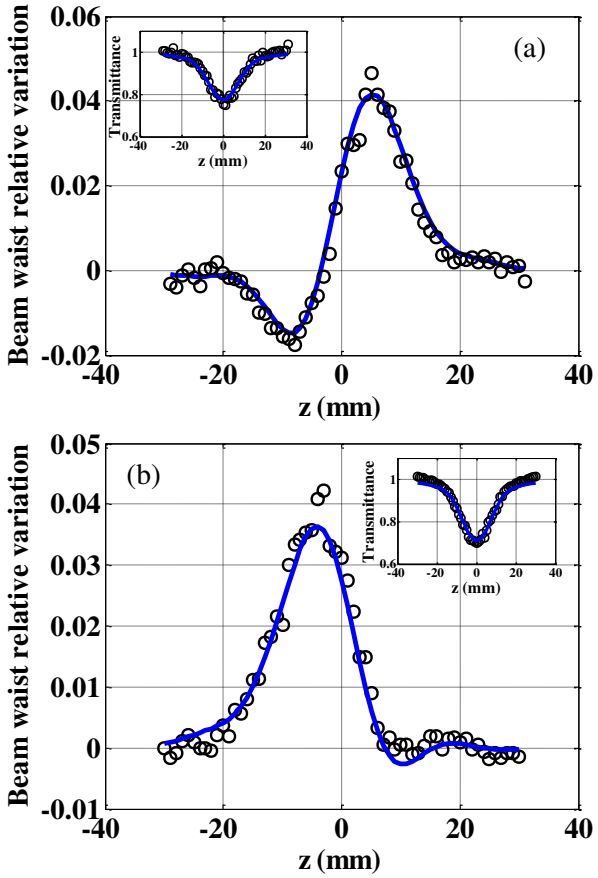

Fig. 1. (Color online): Beam waist relative variation versus z, the sample position at 532 nm. Sample thickness: 1 mm. Pph solution concentration:10^{-3} M. (a) Sample: TPP (α=1126 m^{-1}); (b) sample: ZnTPP (α=1048 m^{-1}). The insets represent the open aperture Z-scan traces and the blue lines represent the best fits of the data.

The BWRV profile shown in Fig. 2(a), with the peak after the valley, indicates that the CoTPP and MCoTPP present a negative n_2 exhibiting self-defocusing at 532nm. Notice that the NLR for both Co-Pphs is relatively small when compared to those shown in Fig. 1 with the same experimental conditions and the same concentration. The normalized transmittances related to the open-aperture Z-scan of these solutions are shown in Fig. 2(b) for CoTPP. The different scans in the figure correspond to different intensities under the same experimental conditions. The transmittance profiles related to the two compounds indicate a saturated absorption behavior. The numerical simulation (in continuous lines) of the experimental data for the normalized transmittance is performed using the squared modulus of Eq. (1).

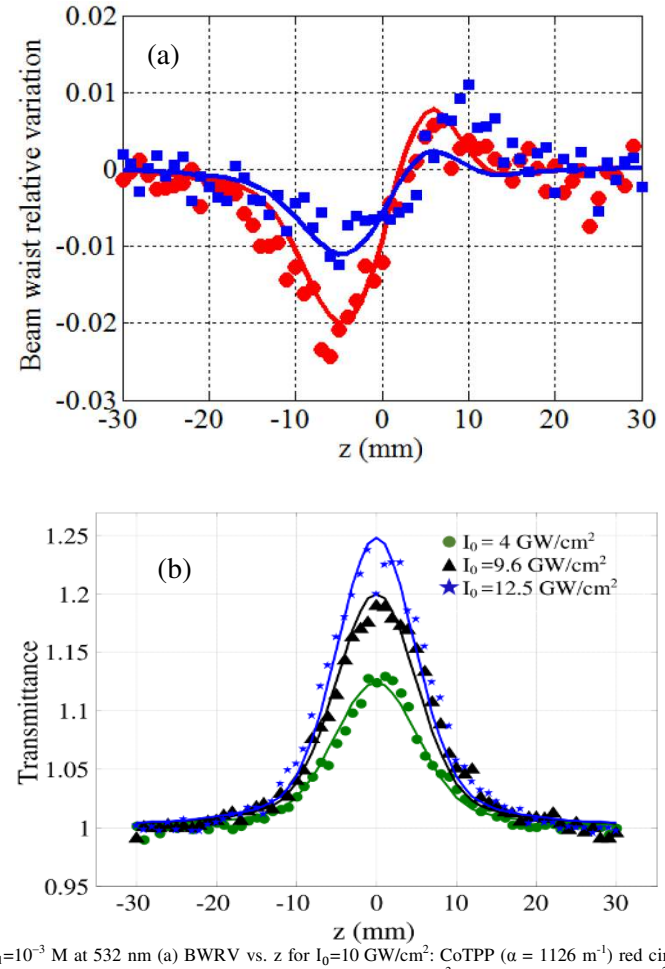

Fig. 2. 1 mm thick solution at $C_1=10^{-3}$ M at 532 nm (a) BWRV vs. z for I_0=10 GW/cm^2: CoTPP (α = 1126 m^{-1}) red circles; MCoTPP (α = 670 m^{-1}) blue squares. (b) NL transmittance vs. z for CoTPP at different intensities (green circles 4 GW/cm^2, black triangles 9.6 GW/cm^2 and blue stars 12.5 GW/cm^2).

The second method used was the DFZ-scan which combines the principles of Dark-field microscopy and the Z-scan method. The use of an annular illumination focused on the tested material, as shown in Fig. 3, provides, through a circular aperture (C_2) at the center of an imaging-magnifying lens (L_2) (5.4x), a NL signal leading to a dark background image on which the observation of the induced NL phase-shift is highly contrasted.

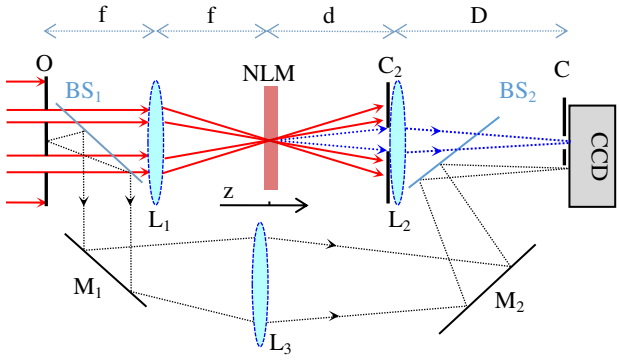

Fig. 3. (Color online): Dark-field Z-scan imaging system. The sample (NLM) is moved along the beam direction around the focal plane. The labels refer to: annular illumination (O), circular apertures (C_2 and C), lenses (L_1, L_2 and L_3), beam splitters (BS_1 and BS_2), CCD camera (CCD) and mirrors (M_1 and M_2).

When compared to Z-scan, the images are spatially resolved and the sensitivity is much higher [4]. Particularly, in our specific experimental setup, it is 60 times larger than the sensitivity of Z-scan in its original version. The annular object has 0.73 mm for the inner disc radius and 1.58 mm for the outer one. The circular aperture C_2 has a radius equal to 0.25 mm. The numerical circular aperture C has a radius 0.454 mm (50 pixels) where the spatial integration allows to calculate the diffracted energy versus z. The sensitivity is highly dependent on these geometrical parameters therefore, the use of a reference material for calibration is recommended. The experimental calibration procedure is very simple and consists in measuring the change of the overall diffracted light in the image plane to allow the detection of a characteristic signal related to known nonlinearities. The diffracted NL signal versus the position of the sample is shown in Fig. 4 obtained at $I_0 = 1.5\ \mathrm{GW/cm^2}$ with 1 mm thick cell of TPP ($1.18x10^{-3}M, \alpha = 1403\ m^{-1}, \beta = 10.8\ \mathrm{cm/GW}$) and ZnTPP ($0.82x10^{-3}M, \alpha = 889\ m^{-1}, \beta = 12.0\ \mathrm{cm/GW}$). For comparison a DF-Zscan trace is plotted with the same experimental conditions for pure CS_2. The results of the fitting confirm the obtained values with the BWRV method at the same concentrations: $n_2 = -3.5\times10^{-18} m^2/W$ for TPP and $n_2 = 1.7\times10^{-18} m^2/W$ for ZnTPP. We emphasize that at this relatively high concentration, it is difficult to extract the NLR signal from the absorption when using classical Z-scan or BWRV configurations. What is important to notice here is the very good agreement shown between the experimental and the simulated profiles in both cases (negative and positive n_2) thus, validating the efficiency of DFZ-scan technique to characterize highly NL absorbing materials. In both cases, the final signal is almost completely due to the NLR. Moreover, the peak after the valley indicates that the TPP presents a negative n_2 exhibiting self-defocusing behavior while, in contrary, the DFZ-scan profile shows self-focusing for the ZnTPP (the valley after the peak). More detailed studies using the DFZ-scan configuration is underway using thin films where the interaction length with the light is very short generating very low NL signal.

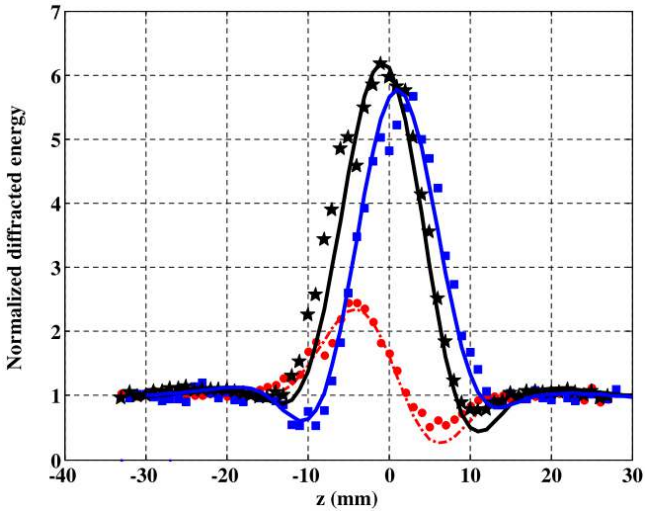

Fig. 4. (color online): Comparison of the normalized diffracted energy versus the position of the sample z using 1 mm thick cell of CS_2 (red) filled circles, TPP (blue) filled squares and ZnTPP (black) filled stars. The lines represent the corresponding simulation ($\lambda = 532$ nm)

Finally, the measured NL parameters for solutions with different concentrations of TPP, ZnTPP, CoTPP and MCoTPP are shown in Table 1 at 532 nm. One can check that the variation of n_2 and β are linear versus the concentration or versus α.

	C (10^{-3}M)	α_{532} (cm^{-1})	I_0 (GW/cm^2)	n_2 ($10^{-18}m^2/W$)	β (cm/GW)
Chlorobenzene			2.0 – 8.0	0.35 ± 0.05	< 0.06
TPP	1	11.2	2.1	-2.7 ± 0.5	5.5 ± 0.8
	0.48	5.45		-0.9 ± 0.3	2.8 ± 0.4
	0.24	2.7		-0.26 ± 0.4	1.3 ± 0.3
	0.12	1.4		0.19 ± 0.1	0.7 ± 0.2
ZnTPP	0.94	10.4	2.1	1.7 ± 0.3	7.8 ± 0.1
	0.47	5.3		0.9 ± 0.2	4.0 ± 0.5
	0.23	2.7		0.6 ± 0.1	2.0 ± 0.3
	0.11	1.1		0.5 ± 0.1	1.0 ± 0.1
CoTPP	0.92	11.2	4.0	-0.4 ± 0.07	-1.5 ± 0.3
	0.53	6.3		-0.1± 0.02	-0.9 ± 0.2
	0.25	3		0.2 ± 0.04	-0.5 ± 0.1
MCoTPP	1	6.7	4.0	-0.01 ± 0.002	-0.7 ± 0.1
	0.7	5		-0.05 ± 0.01	-0.7 ± 0.1
	0.25	1.6		0.1 ± 0.02	-0.2 ± 0.04

Tab. 1. Linear and nonlinear parameters of different Pphs compositions (with different concentrations C), at 532 nm. α_{532} is the linear absorption coefficient, n_2 is the effective NL refractive index, β is the NLA coefficient, I_0 is the laser peak intensity.

At very low concentration ($\alpha \sim 0$), the positive values of n_2 and β in all the cases corresponds to the NL coefficients of pure chlorobenzene (within the experimental errors). Performing the measurements using the solvent alone we found $n_2 = (0.35 \pm 0.05) \times 10^{-18} m^2 / W$ and $\beta < 0.06$ cm/GW. All these compounds were tested using both techniques at 1064 nm at the highest concentration showing no NL responses other than that of the solvent alone.

3. Conclusion

In summary, the solutions were exposed to optical beams at 1064 nm and 532 nm in the picosecond regime using two different methods based on the Z-scan technique. We obtained: i) no response at 1064 nm; ii) at 532 nm there is a change of the sign of n_2 and β depending on the metal incorporated in the free porphyrins. According to [16] this change in the behavior has to be attributed to the *d* shell of the metal (filled or unfilled) incorporated in the free Pphs where the metal with a complete *d* shell (such as zinc) acts as the free TPP for the NLA because its structure is stable. However, cobalt with an incomplete *d* shell acts differently in CoTPP because of the charge transfer between the cobalt *d* shell electrons and the π electrons of the Pphs.

4. Acknowledgments

G. Boudebs and co-workers at LPhiA in Angers would like to acknowledge the organizers of the conference ICL 2017 - Brazil for the invitation to present this work and the financial support from the NNN-TELECOM Program, region des Pays de la Loire. C. B. de Araújo acknowledges financial support from the Brazilian agencies Conselho Nacional de Desenvolvimento Cientifico e Tecnológico (CNPq) and the Fundação de Amparo à Ciência e Tecnologia do Estado de Pernambuco (FACEPE).

References

[1] M. R. Ferdinandus, H. Hu, M. Reichert, D. J. Hagan, E. W. Van Stryland, Opt. Let. 38 (2013) 3518-3521.
[2] K. C. Jorge, H. A. García, A. M. Amaral, A. S. Reyna, L. de S. Menezes, C. B. de Araújo, Opt. Express 23 (2015) 19512-19521.
[3] M. L. Miguez, E. C. Barbano, J. A. Coura, S. C. Zílio, L. Misoguti, Appl. Phys. B 120 (2015) 653-658.
[4] H. Wang, C. Cassagne, H. Leblond, G. Boudebs, Opt. Commun. 366 (2016) 148–153.
[5] G. Boudebs, V. Besse, C. Cassagne, H. Leblond, C. B. de Araújo, Opt. Lett. 38 (2013) 2206-2208.
[6] C. B. de Araújo, A. S. L. Gomes, G. Boudebs, Rep. Prog. Phys. 79 (2016) 036401.
[7] M. Sheik-Bahae, A. A. Said, T. H Wei, D. J. Hagan, E. W. Van Stryland, IEEE J. Quantum Electron 26 (1990) 760-768.
[8] M. O. Senge, M. Fazekas, E. G. A. Notaras, W. J. Blau, M. Zawadzka, O. B. Locos, E. M. Ni Mhuircheartaigh, Adv. Mater. 19 (2007) 2737-2774.
[9] S. Drouet, A. Merhi, D. Yao, M. P. Cifuentes, M. G. Humphrey, M. Wielgus, J. Olesiak-Banska, K. Matczyszyn, M. Samoc, F. Paul, C. O. Paul-Roth, *Tetrahedron*, *68*(50) (2012) 10351-10359.

[10] E. Xenogiannopoulou, M. Medved, K. Iliopoulos, S. Couris, M. G. Papadopoulos, D. Bonifazi, C. Sooambar, A. Mateo-Alonso, M. Prato, *ChemPhysChem*, *8*(7) (2007) 1056-1064.
[11] L. Wang, Y.L. Chen, J.Z. Jiang, *Nanoscale,* **6** (2014) 1871–1878.
[12] M. Zhang, L. Fu, J. Ye, M. G. Humphrey, H. Liu, B. Yan, L. Zhang, J. Shao, C. Zhang, Carbon. **124** (2017) 618-629
[13] N. M. Barbosa Neto, D. S. Correa, L. De Boni, G. G. Parra, L. Misoguti, C. R. Mendonça, I. E. Borissevitch, S. C. Zílio, P. J. Gonçalves, Chem. Phys. Lett. 587 (2013) 118-123.
[14] B. Wang, L. Zhang, B. Li, Y. Li, Y. Shi, T. Shi, Sensors and Actuators B 190 (2014) 93-100.
[15] X. Jin, G. Shi, M. Shui, C. W. Li, J. Y. Yang, X. R. Zhang, Y. X. Wang, K. Yang, Y. L. Song, Chem. Phys. Lett. 489 (2010) 259-262.
[16] D. Swain, A. Rana, P. K. Panda, S. V. Rao, Chem. Phys. Lett. 610 (2014) 310-315.